Statistical properties of two particle systems in a rectangular box: Molecular dynamics simulations

Soong-Hyuck Suh[1,*] and Soon-Chul Kim[2,†]
[1]*Department of Chemical Engineering, Keimyung University, Taegu, 704-701 Korea*
[2]*Department of Physics, Andong National University, Andong 760-749, Korea*
(Received 30 June 2003; revised manuscript received 20 November 2003; published 24 February 2004)

Statistical properties of two particle systems, in which the interaction potentials include the soft repulsion/attraction within a hard rectangular box, are studied using molecular dynamics simulations. The pore size and the potential dependence of van der Waals instability arising from the packing mechanism are investigated. The van der Waals instability strongly depends both on the soft repulsion and on the position of soft attraction in these model systems. An addition of the soft repulsion to the hard-core system gives rise to the van der Waals instability near the position where two particles tend to face each other on the diagonal line of the rectangular box. For the hard-sphere system with the soft repulsion/attractions, the soft attraction significantly enhances the van der Waals instability, whereas, for the square-well spheres with the soft repulsion, the soft attraction reduces the van der Waals instability.

DOI: 10.1103/PhysRevE.69.026111 PACS number(s): 05.10.−a, 61.20.Gy, 64.70.Dv

Phase behavior in a confined system is well known to be influenced by geometrical confinements [1,2]. Much work has been done on layering transition for molecular systems at walls, condensation in pores, and freezing and melting in pores [3–5]. The interesting question is that whether and how the bulk phase transition manifests itself in a finite system because the packing is one of the most important factors controlling the structural properties of the fluid.

For the freezing problem of N hard disks in the two-dimensional circular cavity, Németh and Löwen [6] have carried out computer simulations via the molecular dynamics method, and have shown that the hard disk model exhibits the transition from ergodic to nonergodic behavior at different densities. One important conclusion is that it displays a sequence of ergodicity-breaking and ergodicity-restoring transitions with increasing the area fraction for the system of $\eta_N^l < \eta_N^h$ for $N>7$, where η_N^l and η_N^h denote the lowest and the highest ergodic area fraction, respectively. For a few particles system confined in the circular cavity, however, the solid-liquid transition does not occur, which is related to the transition from ergodic to nonergodic behavior. Strepp *et al.* [7] have recently employed molecular dynamic simulation to investigate the phase transition of hard disks under the periodic external field. Awazu [8] has studied the van der Waals instability of two hard disks in a two-dimensional rectangular box using molecular dynamics simulations, which imitate the solid-liquid transition of the bulk system. For the same model, Munakata and Hu [9] have calculated the exact partition function and the equation of state. They have obtained the similar relationship like the van der Waals equation between the width of the box and the pressure at the side walls. They have also shown that the range of the box width, where the volume compressibility becomes negative, goes to zero when the height of the box passes through the critical value. Comparisons with the results of Nëmeth and Löwen [6] indicate that the van der Waals instability or the phase transition in the confined system is strongly influenced by the geometrical properties of such systems. Most studies in this area are restricted to the systems containing $5-10^3$ particles by Monte Carlo and molecular dynamics simulations.

Many researchers [10–12] have studied the freezing and the glass transition for the three-dimensional hard sphere system confined in a spherical pore. They have shown that the crossover densities for the finite N are found to be significantly smaller than the corresponding bulk densities. On the other hand, recent experimental results and computer simulations for specific models such as supercooled water, liquid carbon, and supercooled silica predict the low-density-liquid (LDL) and the high-density-liquid (HDL) phase [13,14]. It was also shown even in the simple hard-core systems investigated in this work that the presence of the LDL and the HDL in the bulk phase can arises solely from an isotropic interaction potential with characteristic short-ranged attractive/repulsive distances [15]. This result suggests that, for two particle systems with the soft-core repulsion confined in the two-dimensional cavity or the three-dimensional spherical pore, the van der Waals instability may occur because it is not directly related to the transition from ergodic to nonergodic behavior. In particular, Kim and Munakata [16] have more recently studied the statistical properties of two particle systems within the radially symmetric spherical pore. Through theoretical approaches, they have shown that the addition of the soft repulsion to the hard core gives rise to the negative van der Waals instability which is originated from the packing mechanism, while it does not rise the van der Waals instability for the systems with the attractive part of potentials such as the Lennard-Jones fluid. For the two particle system with the soft repulsion in a hard rectangular box, it may occur two different van der Waals instabilities, which are originated from the intermolecular potential between particles and the geometrical properties.

As a model fluid for the two particle system, we have used a simple potential $\phi(r)$ described by

$$\phi(r)=\infty, \quad r<\sigma=\epsilon_1, \quad \sigma<r<\sigma+\sigma_1=\epsilon_2,$$

*Email address: shsuh@kmu.ac.kr
†Email address sckim@andong.ac.kr

$$\sigma+\sigma_1<r<\sigma+\sigma_1+\sigma_2=0, \quad r>\sigma+\sigma_1+\sigma_2. \qquad (1)$$

Here, the model potential in Eq. (1) is reduced to the square-well system for $\epsilon_1<0$ and $\epsilon_2=0$. For $\epsilon_1>0$ and $\epsilon_2=0$, this model becomes the hard-sphere system with the soft repulsion (the HSR model) which was previously employed to investigate the isostructural solid-solid transition [17,18]. For $\epsilon_1>0$ and $\epsilon_2<0$, it becomes the hard-sphere system with both the soft repulsion and the soft attraction (the HSRA model) [15]. For $\epsilon_1<0$ and $\epsilon_2>0$, it becomes the square-well system with the soft repulsion (the HSAR model) which was used to study the influence of short-ranged attractive/repulsive interactions on the phase behavior of colloidal suspensions [19]. It is known that for the bulk system the additions of the repulsive/attractive interactions beyond the hard core may profoundly influence the phase behavior of systems.

We have carried out molecular dynamics (MD) simulations in a manner similar to that originally proposed by Alder and Wainwright for hard-core systems [20]. The width and the height of a hard rectangular box have been taken as a and b, respectively. The hard-wall collisions with the boundaries of the box were treated by the rule of elastic specular scattering, in which the tangential component of velocities to the collision plane was preserved but the normal component of velocities was changed. Postcollisional velocities for colliding particles were also assigned according to specular collision dynamics. Each simulation run was, at a given condition, conducted for a total of 20×10^6 collisional events. Our MD results were all scaled to reduced dimensionless quantities, using the unit hard-disk diameter σ, the particle mass m, and the unit thermal energy k_BT. In this system of units, the translational kinetic energy of the particles in total is scaled to 2, which should be conserved during the MD simulations regardless of the system input parameters for the box size.

It would be interesting to note that quite different effects could emerge in finite systems, which are not observed in the infinite bulk behavior. In the Monte Carlo simulation studies of finite hard spheres confined within a spherical cavity [21], it was reported that the statistical mechanical ensembles were no longer equivalent between the canonical and the grand canonical ensemble simulations. For instance, in certain situations, the significant differences were found in the pore density profiles mainly due to packing constraints. Our MD results are closely related to the canonical ensemble simulations.

The wall pressure diagrams (a vs P_a and a vs P_b) for two square-well spheres with $b=2.1\sigma$ ($\epsilon_1<0$ and $\epsilon_2=0$) are presented in Fig. 1. The pressures at the wall, P_a and P_b, are defined as the time average of the impulse momentum changes by the bouncing of particles on the walls per unit length per unit time. Near the critical width ($\approx2\sigma$) of a rectangular box, where two particles cannot exchange their position, the wall pressure P_a shows the negative compressibility of the van der Waals type imitating the liquid-solid transition in the bulk hard-sphere systems. However, the wall pressure P_b continuously decreases with increasing the wall width a [8,9]. This suggests that under the closely packed situation the van der Waals instability may result from the

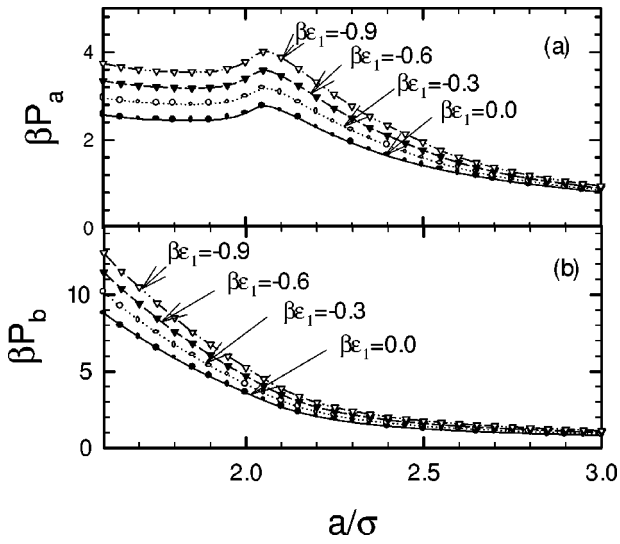

FIG. 1. The wall pressure for two square-well spheres ($\sigma_1=0.5\sigma$ and $\epsilon_2=0$) with $b=2.1\sigma$; (a) P_a and (b) P_b.

structural changes during the packing mechanism. The main difference between two hard-spheres and two square-well spheres is that the negative compressibility of the van der Waals type occurs at the higher pressure with increasing the soft attraction, comparing with the two hard-sphere system. However, the position of the van der Waals instability does not change and appears near the critical width, $a\approx2.05\sigma$. This means that (i) the addition of the soft attraction to hard spheres enhances the wall pressure, and (ii) near the critical width, the van der Waals instability results from the geometrical properties of the rectangular box, not depending on the soft attraction for the hard spheres. This conclusion supports why the van der Waals instability does not exist for two hard-spheres and square-well spheres confined in the spherical hard-wall pore due to the radially symmetric properties [16].

The wall pressure for two hard-spheres with the soft repulsion (the HSR model) with $\sigma_1=0.5\sigma$ is shown in Fig. 2. Our simulation results display the two types of van der Waals instabilities; the first van der Waals instability occurs near $a\approx2.05\sigma$ when two hard spheres approach each other, and the second van der Waals instability near $a\approx2.55\sigma$. As we increase the soft repulsion, the wall pressure P_a decreases, while the wall pressure P_b increases. For two square-well spheres, however, both P_a and P_b increase with increasing the soft attraction. One interesting observation is that the position of the second van der Waals instability appeared near $a\approx2.55\sigma$, not depending on the height of the soft repulsion, even though the second van der Waals instability occurs for highly repulsive systems.

The density profiles $\rho(x,y)$ and the radial distribution functions (RDF's) for the HSR model with $\epsilon_1=0.9$ are presented in Fig. 3. The contact density distribution $\rho(x,y=0)$ at the lower and upper walls also shows the two peaks near $a\approx2.05\sigma$ and $a\approx2.55\sigma$, while the contact density distribution $\rho(x=0,y)$ at the side walls continuously decreases with increasing the wall width a. Under those conditions the wall pressure itself satisfies the contact value theorem which is

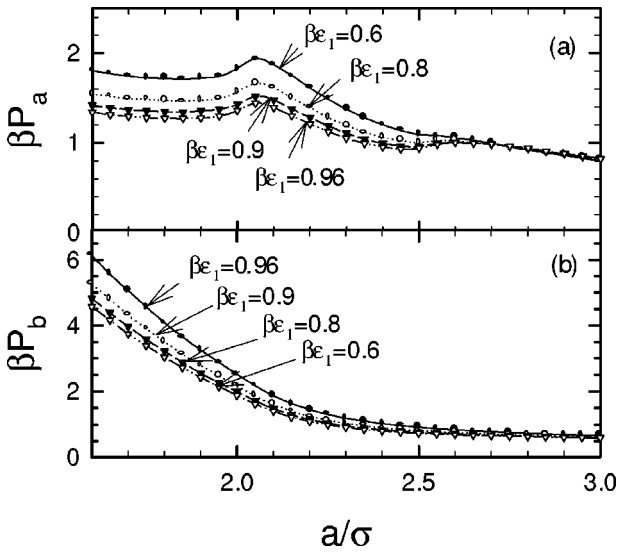

FIG. 2. The wall pressure for two hard spheres with the soft repulsion (the HSR model) ($\sigma_1=0.5\sigma$ and $\epsilon_2=0$) with $b=2.1\sigma$; (a) P_a and (b) P_b.

related to the density distribution on the wall [2,22]. Two types of van der Waals instabilities can be understood as the arrangement of two hard spheres with the soft repulsion in a rectangular box. When the width of a box at the fixed side wall ($b=2.1\sigma$) is larger than the particle size, two particles tend to arrange along the horizontal line of a rectangular box. In this case, the impulse momentum change at the side walls is greater than that of the upper or lower walls. When the size of the side walls a is reduced, two particles tend to face each other on a diagonal line of the rectangular box, and the wall pressure is strongly affected by the soft repulsion interaction ($\epsilon_1>0$). Finally, when the side wall is further reduced, two particles tend to face each other on a vertical line of a rectangular box and the hard sphere interaction strongly influences on the wall pressure. Such structural properties were confirmed from the radial distribution functions, defined as the two-particle probability as a function of the relative distance r. The RDF's obtained from our simulations are illustrated in Fig. 3(c), and the profound structural changes are displayed near $r/\sigma=0.5$ due to the repulsive potential in the HSR model. This implies that the second van der Waals instability appears at the position where two particles tend to face each other on the diagonal line of a rectangular box, depending on the soft repulsion of model potentials.

Figure 4 illustrates the wall pressure P_a ($\epsilon_1=0.9$ and $b=2.1\sigma$) for the HSR model with the different repulsive shoulder. Once again, the position of the first van der Waals instability exactly coincides with that of two hard spheres. However, the position of the second van der Waals instability appears over the large a value with increasing the width of the soft repulsion, even though the wall pressure decreases with increasing the soft repulsion, i.e., with increasing the width of the repulsive shoulder. Comparison with Figs. 2 and 3 indicates that the position of the second van der Waals instability only depends on the width σ_1 of the repulsive shoulder (or the range of the soft repulsion), but not the height of the soft repulsion ϵ_1. Here, one question is how to

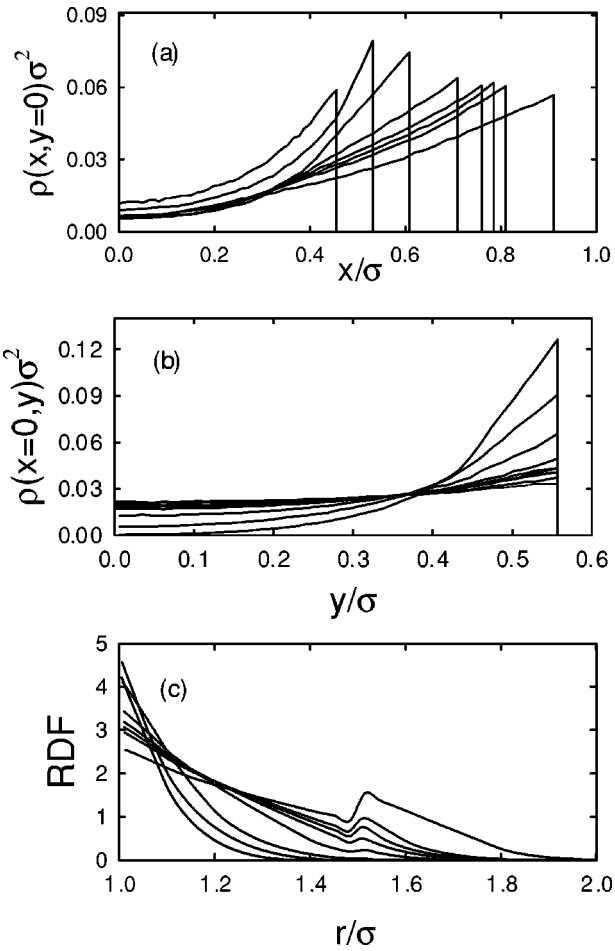

FIG. 3. The contact density profile ρ at the wall, and the radial distribution function, RDF, for the HSR model ($\sigma_1=0.5\sigma$ and $\epsilon_2=0$) with $b=2.1\sigma$; (a) $\rho(x,y=0)\sigma^2$ (from left to right, $a=1.9\sigma$, $a=2.05\sigma$, $a=2.2\sigma$, $a=2.4\sigma$, $a=2.5\sigma$, $a=2.55\sigma$, $a=2.6\sigma$, and $a=2.8\sigma$), (b) $\rho(x=0,y)\sigma^2$ [the conditions for a are the same as in (a) but from top to bottom at the wall], and (c) RDF [the conditions for a are the same as in (a) but from left to right].

interpret the second van der Waals instability. It is known that for the bulk model systems with the purely repulsive interactions the liquid-gas transition does not exist. In such systems, there is no distinction between the gas and the liquid phases and the liquid-gas transition results mainly from the attractive force between two particles.

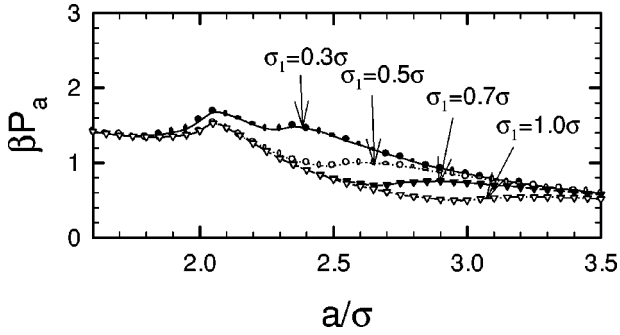

FIG. 4. The wall pressure P_a for the HSR model ($\epsilon_1=0.9$ and $\epsilon_2=0$) with $b=2.1\sigma$.

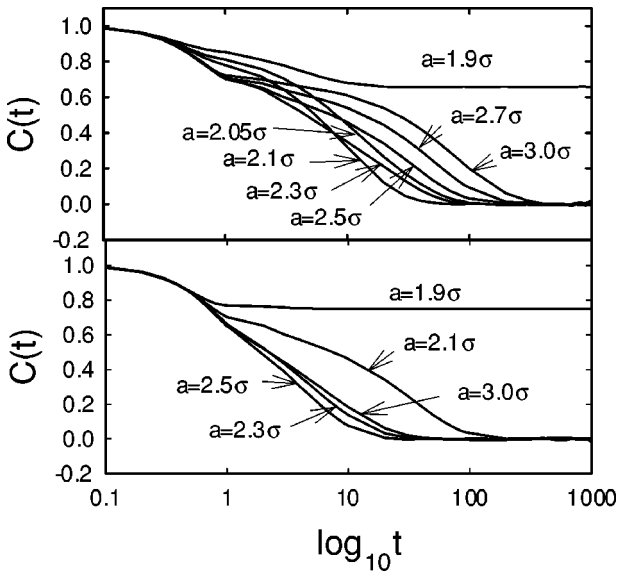

FIG. 5. The position autocorrelation function $C(t)$ for the HSR model ($\epsilon_1=0.9$, $\sigma_1=0.5\sigma$, and $\epsilon_2=0$); (a) $b=2.1\sigma$ and (b) $b=2.5\sigma$.

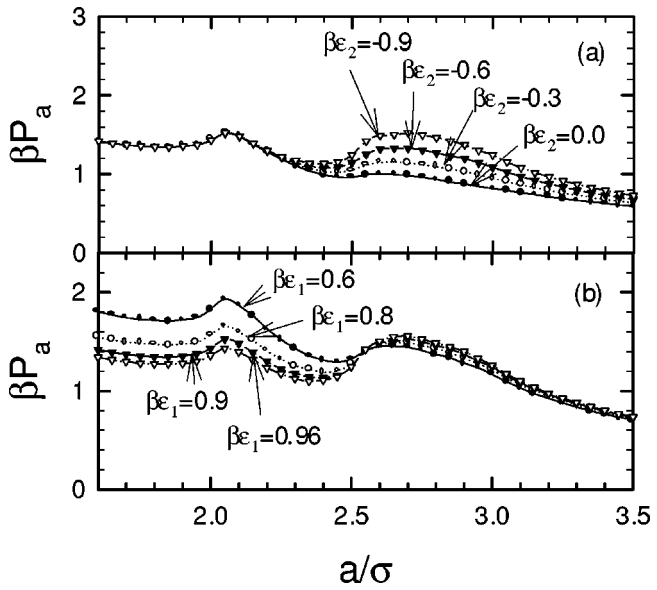

FIG. 6. (a) The wall pressure P_a for the HSRA model ($\epsilon_1=0.9$, $\sigma_1=0.5\sigma$, and $\sigma_1=0.5\sigma$) with $b=2.1\sigma$. (b) The wall pressure P_a for the HSRA model ($\epsilon_2=-0.9$, $\sigma_1=0.5\sigma$, and $\sigma_1=0.5\sigma$) with $b=2.1\sigma$.

To understand the detailed dynamic properties of the van der Waals instabilities, the autocorrelation functions for the position of each particle were illustrated in Fig. 5. The position autocorrelation function $C(t)$ is defined as

$$C(t)=\frac{\langle \mathbf{x}(0)\mathbf{x}(t)\rangle}{\langle \mathbf{x}(0)\mathbf{x}(0)\rangle}, \tag{2}$$

where $\mathbf{x}(t)$ is the position of particle at a given time t. In the solid state, the position autocorrelation function has a nonzero finite value for $t\rightarrow\infty$. In this case, two particles in a rectangular box cannot exchange their positions each other. In the liquid state, the faster relaxation is expected to be processed which is not observed in the case of the solid state. As can be seen in Fig. 5, the relaxation process becomes slower when the width of the box a approaches closer to the first van der Waals instability ($a\approx 2.05\sigma$). For the wide wall ($b=2.5\sigma$), the position autocorrelation function converges very rapidly as the width of the box increases. An interesting observation can be found in the case of the narrow wall ($b=2.1\sigma$). In this condition and near the first van der Waals instability, the position autocorrelation function converges very rapidly such as purely hard sphere systems [8]. However, near the second van der Waals instability, the time in which the autocorrelation approaches to zero becomes longer than the first van der Waals instability. These curves also show the fast and the slow relaxations for a little above and below the second van der Waals instability ($a\approx 2.55\sigma$). These relaxations are similar to the α- and β- relaxation of the density fluctuation in a supercooled liquid [8,23]. The fast and the slow relations are separated by the appearance of plateau. The liquid state above the second van der Waals instability ($a>2.55\sigma$) is different from that below the second van der Waals instability ($2.05\sigma<a<2.55\sigma$) as detected in the HDL and the LDL. From this observation, we may suggest that (i) our two particles system may imitate the bulk liquid-liquid phase transition in the system consisting of many particles and (ii) the addition of the soft repulsion to the hard core can give rise to the van der Waals instability.

For the HSRA model with the soft repulsion ($\epsilon_1>0$) and the soft attraction ($\epsilon_2<0$), the pressure P_a and the position autocorrelation function $C(t)$ obtained from our simulations are illustrated in Figs. 6 and 7, respectively. Figure 6 indicates that the addition of the soft attraction enhances the second van der Waals instability. However, the positions of the van der Waals instabilities exactly coincide with that of the HSR model as shown in Figs. 3 and 4. Even though we did not display the density distribution $\rho(x,y)\sigma^2$ in these figures, the sharp and narrow density distributions near the van der Waals instabilities are observed as in the HSR mode. The density enhancement near the van der Waals instability can be understood by considering the role of the soft attraction. This result confirms that the position of the second van der Waals instability only depends on the width of the repulsive shoulder, but not the soft attraction. We can conclude

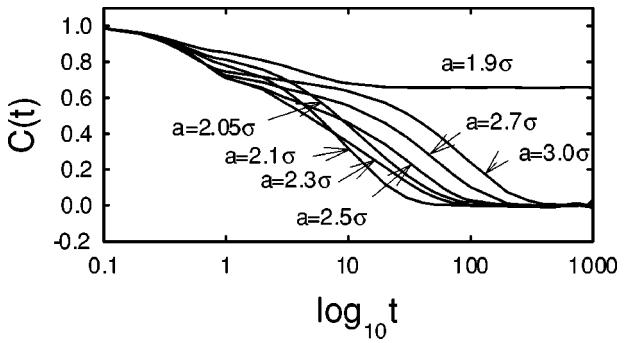

FIG. 7. The position autocorrelation function $C(t)$ for the HSRA model ($\epsilon_1=0.9$, $\epsilon_2=-0.9$, $\sigma_1=0.5\sigma$, and $\sigma_2=0.5\sigma$) with $b=2.1\sigma$.

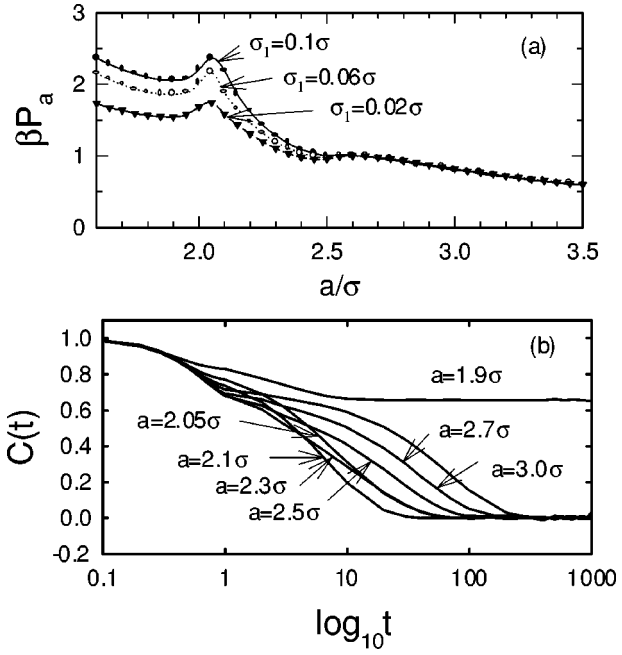

FIG. 8. (a) The wall pressure P_a for the HSAR model ($\epsilon_1=-0.05$, $\epsilon_2=0.96$, and $\sigma_2=0.5\sigma$) with $b=2.1\sigma$. (b) The position autocorrelation function $C(t)$ ($\epsilon_1=-0.05$, $\epsilon_2=0.96$, $\sigma_1=0.02\sigma$, and $\sigma_2=0.5\sigma$) with $b=2.1\sigma$.

that the addition of the soft attraction to the HSR model enhances the van der Waals instability which is somewhat similar to the liquid-liquid phase transition in the bulk system. We can also check the contribution of the soft repulsion from the position autocorrelation function (Fig. 7). Near the second van der Waals instability, the HSRA model leads to the slower relaxation compared with the HSR model, while near the first van der Waals instability the faster relaxation is detected. The soft attraction in the HSRA model results in the slower relaxation. This can be understood by considering the effect of the soft attraction in the packing mechanism. This enhancement is similar with the solid-solid enhancement of the bulk system [18]. The addition of the soft repulsion to the square well gives rise to the liquid-liquid transition. It is noted that the combination of narrow attractive square well with the repulsive square-shoulder potential would enhance the stability of isostructural solid-solid transition over the system of the square-well potential alone [19].

Furthermore, in order to understand the role of the soft attraction for the van der Waals instability, we have considered two square-well spheres with the soft repulsion (the HSAR model). The wall pressure and the position autocorrelation function were displayed in Fig. 8. For two square-well spheres (the HSAR model with $\epsilon_2=0$), the second van der Waals instability does not exist. In this case, it is expected that for the weak repulsion the soft attraction overcomes the soft repulsion and the second van deer Waals instability eventually disappears. As we increases the width of the repulsive shoulder (or the soft attraction), the position of the second van der Waals instability moves to higher a values. The wall pressure near the first van der Waals instability increases, but decreases near the second ven der Waals instability. Comparison with Fig. 7 indicates that the position of the second van der Waals instability strongly depends on the position of the soft repulsion as well as the width of the soft repulsion. This result again confirms that the second van der Waals instability is directly related to the soft repulsion of model potentials, while the addition of the soft repulsion to the square-well system enhances the second van der Waals instability. The general trend for the position autocorrelation function for the HSAR model as shown in Fig. 8(b) is very similar with that of the HSR model (Fig. 7) except for the faster relaxation near the second van der Waals instability. From these figures we observe the following. (i) In the solidlike state, the position autocorrelation functions have a finite positive value because two particles cannot exchange their positions, (ii) the position autocorrelation functions drop off rapidly in the fluidlike state where particle positions are available over all configurational space, and (iii) in the intermediate range between the solid and fluid states, the position autocorrelation functions exhibit a plateau due to relaxation processes resulting from the collisions between two particles. These time-dependent functions also explain that the soft attraction in the HSAR model reduces the second van der Waals instability. The overall picture shows that the van der Waals instabilities are strongly affected by the position of soft attraction of model potentials.

In summary, we have considered many different potential models to study the van der Waals instability arising from the packing mechanism. The van der Waals instabilities are affected not only by the soft repulsion but also by the position of the soft attraction in model potentials. For two hard spheres in the spherical pore [24], the van der Waals instability related to the solid-liquid transition in the bulk system does not occur mainly due to the geometrical properties of a spherical symmetry. However, the present result suggests that two hard ellipsoids in the hard spherical pore may give rise to the two types of van der Waals instabilities as observed in the system of two hard spheres with the soft repulsion [25]. It is expected that the van der Waals instability in the confined systems can also be affected by the wall potential, e.g., nitrogen in zeolite systems [26]. It would be interesting to study the statistical properties of two hard ellipsoids in the two-dimensional rectangular box or the spherical pore and we will discuss these problems in the near future.

This work was in part supported by Korea Research Foundation Grant (Grant No. KRF-2003-015-C00230) and the KOSEF.

[1] R. Evans, in *Fundamentals of Inhomogeneous Fluids*, edited by D. Henderson (Marcel Dekker, New York, 1992); H. Löwen, Phys. Rep. **237**, 249 (1994).

[2] H.T. Davis, *Statistical Mechanics of Phases, Interfaces, and Thin Films* (VCH, New York, 1996).

[3] L.D. Gelb, K.E. Gubbins, R. Radhakrishnan, and M. Sliwinska-Bartkowiak, Rep. Prog. Phys. **62**, 1573 (1999).

[4] H.K. Christenson, J. Phys.: Condens. Matter **13**, R95 (2001).

[5] C. Bechinger, Curr. Opin. Colloid Interface Sci. **7**, 204 (2002).
[6] Z.T. Nëmeth and H. Löwen, J. Phys.: Condens. Matter **10**, 6189 (1998).
[7] W. Strepp, S. Sengupta, and P. Nielaba, e-print cond-mat/029363.
[8] A. Awazu, Phys. Rev. E **63**, 032102 (2001).
[9] T. Munakata and G. Hu, Phys. Rev. E **65**, 066104 (2002).
[10] S.T. Chui, Phys. Rev. B **43**, 11 523 (1991).
[11] Z.T. Nëmeth and H. Löwen, Phys. Rev. E **59**, 6824 (1999).
[12] W.K. Kegel, J. Chem. Phys. **115**, 6538 (2001); W.K. Kegel, H. Reiss, and H.N.W. Lekkerkerker, Phys. Rev. Lett. **83**, 5298 (1999).
[13] Y. Katayama, T. Mizutama, W. Utzumi, O. Shimomura, Y. Yamakata, and K. Funakoshi, Nature (London) **403**, 170 (2000), and references therein.
[14] E.A. Jagla, Phys. Rev. E **63**, 061501 (2001).
[15] G. Malescio, G. Franzese, G. Pellicana, A. Skibinsky, S.V. Buldyrev, and H.E. Stanley, J. Phys.: Condens. Matter **14**, 2193 (2002).
[16] S.-C. Kim and T. Munakata, J. Korean. Phys. Soc. **43**, 997 (2003).
[17] J.M. Kincaid, G. Stell, and E. Goldmark, J. Chem. Phys. **65**, 2172 (1976).
[18] A.R. Denton and H. Löwen, J. Phys.: Condens. Matter **9**, L1 (1997); C.N. Likos, Z.T. Nëmeth and H. Löwen, *ibid.* **6**, 10 965 (1994); P. Bolhuis and D. Frenkel, Phys. Rev. Lett. **72**, 2211 (1994).
[19] A.R. Denton and H. Löwen, J. Phys.: Condens. Matter **9**, 8907 (1997); E.J.W. Verwey and J.T.G. Overbeek, J. Colloid Interface Sci. **172**, 425 (1994).
[20] B.J. Alder and T.E. Wainwright, J. Chem. Phys. **31**, 459 (1959); M.P. Allen and D.J. Tildesley, *Computer Simulation of Liquids* (Clarendon Press, Oxford, 1987).
[21] A. González, J.A. White, F.L. Román, and R. Evans, J. Chem. Phys. **109**, 3637 (1998).
[22] D. Henderson, L. Blum, and J.L. Lebowitz, J. Electroanal. Chem. **102**, 315 (1979).
[23] W. Götze and L. Sjögren, Rep. Prog. Phys. **55**, 241 (1992).
[24] J.A. White, A. González, F.L. Román, and S. Velasco, Phys. Rev. Lett. **84**, 1220 (2000).
[25] M. Calleja and G. Rickayzen, J. Phys.: Condens. Matter **7**, 8839 (1995).
[26] T.J. Grey, J.D. Gale, and D. Nicholson, in *Fundamentals of Adsorption-7*, edited by F. Meunier (Elsevier, Paris, 2002), p. 360.